

# Maintaining a Resonance Condition of an RF Spin Rotator Through a Feedback Loop in a Storage Ring

V. Hejny,<sup>1</sup> A. Andres,<sup>2,1,\*</sup> J. Pretz,<sup>2,1</sup> F. Abusaif,<sup>2,1,†</sup> A. Aggarwal,<sup>3</sup> A. Aksentev,<sup>4</sup> B. Alberdi,<sup>2,1,‡</sup> L. Barion,<sup>5</sup> I. Bekman,<sup>1,§</sup> M. Beyß,<sup>2,1</sup> C. Böhme,<sup>1</sup> B. Bretkreutz,<sup>1</sup> N. Canale,<sup>5</sup> G. Ciullo,<sup>5</sup> S. Dymov,<sup>5</sup> N.-O. Fröhlich,<sup>1,¶</sup> R. Gebel,<sup>1</sup> M. Gaisser,<sup>2</sup> K. Grigoryev,<sup>1,\*</sup> D. Grzonka,<sup>1</sup> J. Hetzel,<sup>1,\*</sup> O. Javakhishvili,<sup>6,||</sup> A. Kacharava,<sup>1</sup> V. Kamerdzhev,<sup>1,\*</sup> S. Karanth,<sup>3</sup> I. Keshelashvili,<sup>1,\*</sup> A. Kononov,<sup>5</sup> K. Laihem,<sup>2,\*</sup> A. Lehrach,<sup>2,1</sup> P. Lenisa,<sup>5</sup> N. Lomidze,<sup>7</sup> B. Lorentz,<sup>8</sup> G. Macharashvili,<sup>7</sup> A. Magiera,<sup>3</sup> D. Mchedlishvili,<sup>7</sup> A. Melnikov,<sup>4</sup> F. Müller,<sup>2,1</sup> A. Nass,<sup>1</sup> N.N. Nikolaev,<sup>9</sup> D. Okropiridze,<sup>7,\*\*</sup> A. Pesce,<sup>1</sup> A. Piccoli,<sup>5</sup> V. Poncza,<sup>1</sup> D. Prasuhn,<sup>1</sup> F. Rathmann,<sup>1,††</sup> A. Saleev,<sup>5,‡‡</sup> D. Shergelashvili,<sup>7</sup> V. Shmakova,<sup>5,††</sup> R. Shankar,<sup>5</sup> N. Shurkhno,<sup>1,\*</sup> S. Siddique,<sup>2,1,\*</sup> A. Silenko,<sup>10</sup> J. Slim,<sup>2,¶</sup> H. Soltner,<sup>11</sup> R. Stassen,<sup>1</sup> E.J. Stephenson,<sup>12</sup> H. Ströher,<sup>1</sup> M. Tabidze,<sup>7</sup> G. Tagliente,<sup>13</sup> Y. Valdau,<sup>1,\*</sup> M. Vitz,<sup>2,1</sup> T. Wagner,<sup>2,1,\*</sup> A. Wirzba,<sup>14</sup> A. Wrońska,<sup>3</sup> P. Wüstner,<sup>11</sup> and M. Žurek<sup>1,§§</sup>

(JEDI collaboration)

<sup>1</sup>*Institut für Kernphysik, Forschungszentrum Jülich, 52425 Jülich, Germany*

<sup>2</sup>*III. Physikalisches Institut B, RWTH Aachen University, 52056 Aachen, Germany*

<sup>3</sup>*Marian Smoluchowski Institute of Physics, Jagiellonian University, 30348 Cracow, Poland*

<sup>4</sup>*Institute for Nuclear Research, Russian Academy of Sciences, 117312 Moscow, Russia*

<sup>5</sup>*University of Ferrara and Istituto Nazionale di Fisica Nucleare, 44100 Ferrara, Italy*

<sup>6</sup>*Department of Electrical and Computer Engineering, Agricultural University of Georgia, 0159 Tbilisi, Georgia*

<sup>7</sup>*High Energy Physics Institute, Tbilisi State University, 0186 Tbilisi, Georgia*

<sup>8</sup>*GSI Helmholtzzentrum für Schwerionenforschung, 64291 Darmstadt, Germany*

<sup>9</sup>*L.D. Landau Institute for Theoretical Physics, 142432 Chernogolovka, Russia*

<sup>10</sup>*Bogoliubov Laboratory of Theoretical Physics, International Intergovernmental Organization Joint Institute for Nuclear Research, 141980 Dubna, Russia*

<sup>11</sup>*Institute of Technology and Engineering, Forschungszentrum Jülich, 52425 Jülich, Germany*

<sup>12</sup>*Indiana University, Department of Physics, Bloomington, Indiana 47405, USA*

<sup>13</sup>*Istituto Nazionale di Fisica Nucleare sez. Bari, 70125 Bari, Italy*

<sup>14</sup>*Institute for Advanced Simulation, Forschungszentrum Jülich, 52425 Jülich, Germany*

(Dated: January 30, 2025)

This paper presents the successful application of a phase-lock feedback system to maintain the resonance condition of a radio frequency (rf) spin rotator (specifically, an rf Wien filter) with respect to a 120 kHz spin precession in the Cooler Synchrotron (COSY) storage ring. Real-time monitoring of the spin precession and the rf Wien filter signal allows the relative phase between the two to be stabilized at an arbitrary setpoint. The feedback system compensates for deviations in the relative phase by adjusting the frequency and/or phase as needed. With this method, a variation in phase relative to the demand phase with a standard deviation of  $\sigma_{\Delta\varphi} \approx 0.2$  rad could be achieved. The system was implemented in two runs aiming at a first direct measurement of the deuteron electric dipole moment in 2018 and 2021. In addition, the difference between a single-bunch beam affected by the spin rotator and a two-bunch system in which only one bunch is exposed to the spin rotator fields is discussed. Both methods have been used during these beam times. The ability to keep the spin precession and the rf fields synchronized is also crucial for future investigations of electric dipole moments of charged particles using storage rings.

## I. MOTIVATION

Radio Frequency (rf) spin rotators are essential devices used in particle accelerators, specifically storage rings, to

\* Present address: GSI Helmholtz Centre for Heavy Ion Research, 64291 Darmstadt, Germany

† Present address: Karlsruhe Institute of Technology, Hermann-von-Helmholtz-Platz 1, 76344 Eggenstein-Leopoldshafen, Germany

‡ Present address: Humboldt-Universität zu Berlin, Institut für Physik, Newton-Strasse 15, 12489 Berlin, Germany

§ Present address: Institute of Technology and Engineering, Forschungszentrum Jülich, 52425 Jülich, Germany

¶ Present address: Deutsches Elektronen-Synchrotron, 22607 Hamburg, Germany

|| Present address: Faculty of Nuclear Sciences and Physical Engineering, Czech Technical University in Prague, 160 00 Praha 6,

Czech Republic

\*\* Present address: Ruhr-Universität Bochum, Institut für Experimentalphysik I, 44801 Bochum, Germany

†† Present address: Brookhaven National Laboratory, Upton, NY 11973, USA

‡‡ Present address: Institut für nachhaltige Wasserstoffwirtschaft, Forschungszentrum Jülich, 52425 Jülich, Germany

§§ Present address: Argonne National Laboratory, Lemont, Illinois 60439, USA

manipulate the spin orientation of particles such as protons, electrons, or polarized ions. By generating oscillating magnetic and/or electric fields, these devices interact with the particle's magnetic moment, allowing precise control over the spin direction ideally without affecting the particle's trajectory. This control is crucial for precision experiments in nuclear and particle physics, where spin polarization plays a significant role in probing fundamental interactions.

Rf spin rotators have to run on resonance with the spin precession, *i.e.* the oscillation frequency  $f_{\text{rf}}$  has to be a harmonic of the spin precession frequency  $f_s$ . Using the spin tune  $\nu_s = \gamma G$  (with  $\gamma$  and  $G$  being the Lorentz factor and the gyromagnetic anomaly, respectively) one can write

$$f_{\text{rf}} = |\nu_s + h| f_{\text{rev}}, \quad h \in \mathbb{Z}, \quad (1)$$

where  $f_{\text{rev}}$  is the revolution frequency of the beam.  $|\nu_s| = f_s/f_{\text{rev}}$  also describes the number of spin revolutions per turn. As the stability of  $\nu_s$  depends on a multitude of storage-ring parameters, the question arises whether a constant frequency  $f_{\text{rf}}$  is sufficient for maintaining this resonance condition. This paper discusses this issue in the context of recent experimental efforts at the Cooler Synchrotron COSY at Forschungszentrum Jülich.

The JEDI collaboration (Jülich Electric Dipole Moment Investigations) has installed a novel wave-guide rf Wien filter[1, 2] at COSY with the aim of conducting a first direct measurement of the permanent electric dipole moment (EDM) of the deuteron. The existence of such an EDM would be an essential ingredient in explaining one of the unsettled questions in particle physics and cosmology: the dominance of matter over anti-matter in the universe, quantified by the parameter  $\eta = (n_B - n_{\bar{B}})/n_\gamma$ [3], which exceeds the Standard Model predictions by several orders of magnitude.

In the absence of an EDM, the invariant spin axis in an ideal magnetic storage ring is vertical, resulting in the spin precession within the ring plane. A non-zero EDM causes a tilt of the invariant spin axis, leading to a small oscillation of the vertical spin component. The experimental approach employs the rf Wien filter to accumulate these spin rotations[4–6]. The magnitude of the resulting signal depends on the relative phase  $\varphi_{\text{rel}}$  of the spin precession and the field oscillations in the rf Wien filter. This dependence of the experimental signal on  $\varphi_{\text{rel}}$  requires the ability to set and control this phase along with the resonance condition in real time.

This paper presents a control system for phase and frequency implemented at COSY for the experimental runs with the rf Wien filter in 2018 and 2021. A proof of principle of a similar system has already been reported in [7]. However, that approach was different: instead of the frequency signal  $f_{\text{rf}}$  the beam revolution frequency  $f_{\text{rev}}$  had been controlled to stabilize and control the spin precession itself. The solution discussed here, *i.e.* modifying  $f_{\text{rf}}$  and its phase, was chosen to avoid higher-order effects for other beam parameters. Two scenarios are presented:

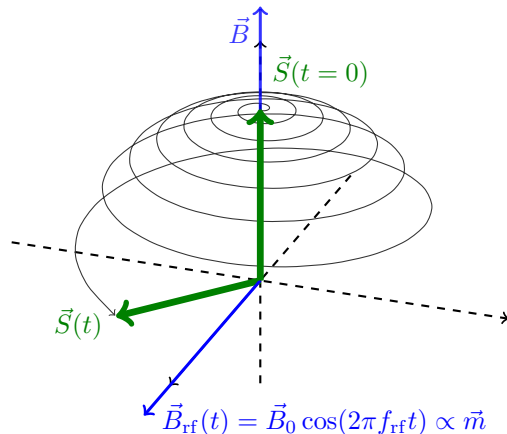


FIG. 1. As an example, the initial spin vector  $\vec{S}(t=0)$  points in vertical direction. An rf device providing a magnetic field  $\vec{B}_{\text{rf}}(t) = \vec{B}_0 \cos(2\pi f_{\text{rf}} t)$  with  $\vec{B}_0 = B_0 \vec{m}$  then rotates the spin vector by an angle  $\chi(t) \propto B_{\text{rf}}(t)$  per pass around the axis  $\vec{m} \parallel \vec{B}_0$ , see Eq. (2). In addition, the holding field  $\vec{B}$  of the accelerator causes the spin vector to precess with the frequency  $f_s = \nu_s f_{\text{rev}}$  around the vertical axis. This only works if the resonance condition in Eq. (1) is satisfied.

one where the feedback system acts directly on a particle bunch influenced by the rf spin rotator, and another employing two bunches and a newly developed system with fast switches to operate the rf spin rotator selectively on a specific bunch [8] with the feedback acting on the second, unaffected bunch. An analytic model is used to discuss the differences between the two use cases.

## II. INTRODUCTION

For the following discussion on spin rotations, the effects of an electric dipole moment (EDM) are neglected. Furthermore, the term "polarization" is used instead of "spin". Polarization, defined as the statistical average of individual spin vectors, is the measurable representation of the collective spin state of the particles. Strictly speaking, a spin rotator acts on the individual spins. However, the polarization vector follows the same rules. All important variables used in the following sections are listed in Tables I and II.

The polarization vector in a storage ring is comprised of two main components: a stable component parallel to the invariant spin axis  $\vec{c}$ , and a precessing component in the plane perpendicular to it. In the case of an ideal magnetic ring without any additional spin rotators, the invariant spin axis is vertical, *i.e.* parallel to the magnetic field of the bending elements. Typical observables include the vertical and in-plane components of the polarization,  $p_v$  and  $p_h$ , respectively, as well as the spin tune,  $\nu_s$ . In recent years, the JEDI collaboration has developed tools to measure these quantities in real-time

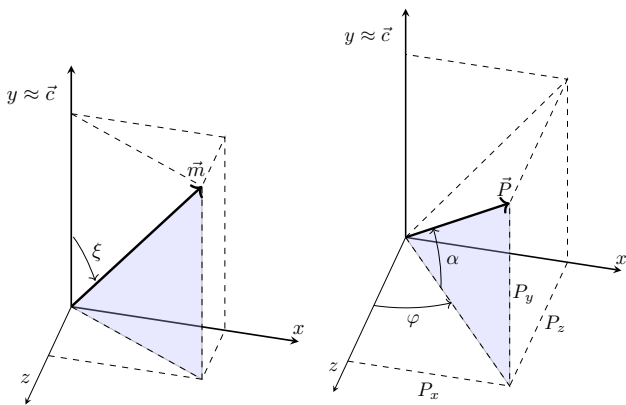


FIG. 2. Left: Definition of angle  $\xi$ ,  $\vec{c}$  denotes the invariant spin axis, which deviates only by a small amount from the vertical direction. A spin rotator rotates the spin vector around the axis  $\vec{m}$ . Right: Definition of angles  $\alpha$  and  $\varphi$ .

with high precision [7, 9–11].

An rf spin rotator can be characterized by a rotation axis  $\vec{m}$  (defined by the oscillating magnetic and/or electric fields), an oscillation frequency  $f_{\text{rf}}$ , an initial phase  $\varphi_{\text{rf}}$  at  $t = 0$ , and a rotation angle per pass

$$\chi(t) = \chi_0 \sin(2\pi f_{\text{rf}} t + \varphi_{\text{rf}}). \quad (2)$$

If one assumes a bunched beam with bunches passing the rf spin rotator at times  $t = n/f_{\text{rev}}$  (with  $n \in \mathbb{N}$  being the turn number), this becomes

$$\chi(n) = \chi_0 \sin(2\pi\nu_s n + \varphi_{\text{rf}}) \quad (3)$$

if the resonance condition given in Eq. (1) is fulfilled. The most basic scenario is a rotation out of the stable, non-precessing vertical spin direction as shown exemplarily in Fig. 1 resulting in an oscillation of the vertical polarization component  $p_v$  with the frequency  $f_v$ . Other cases depend on the relative phase between the spin precession and  $f_{\text{rf}}$ . One can define the resonance spin-flip tune (or resonance strength)  $\epsilon$  as

$$\epsilon = \frac{f_v}{f_{\text{rev}}} = \frac{1}{4\pi} \chi_0 |\vec{c} \times \vec{m}| = \frac{1}{4\pi} \chi_0 \sin \xi \quad (4)$$

with  $\xi$  being the tilt angle of the rotation axis with respect to the invariant spin axis, as shown in Fig. 2 [12]. Thus, the resonance strength is a direct measure of the tilt angle  $\xi$ .

In order to decide on the necessity of an active frequency and phase control, one needs to consider the impact of a detuned frequency as well as the phase stability. Running off-resonance by a frequency change  $\Delta f$  has a direct impact on the induced spin motion. For example, as shown in Sect. V A, Eq. (33), the amplitude of the oscillating polarization can be described by a Lorentz curve with the width  $\Gamma = 2\epsilon f_{\text{rev}}$ . Thus, as a first criterion, if the variation of the spin precession frequency  $f_s$  over the running period is of similar size or larger, one needs to

adjust  $f_{\text{rf}}$  with time. For the operation of the rf Wien filter at COSY typical run-time parameters are (see [6])

$$\chi_0 \approx 3.8 \times 10^{-6} \text{ rad} \quad (5)$$

$$\xi \approx -30 \text{ mrad to } 30 \text{ mrad} \quad (6)$$

$$f_{\text{rev}} \approx 750\,000 \text{ Hz}, \quad (7)$$

resulting in  $\Gamma < 13.6 \text{ mHz}$ . The typical variation of the spin tune within one cycle is  $\Delta\nu_s \approx 10^{-8}$  [10] corresponding to  $\Delta f_s \approx 7.5 \text{ mHz}$ .

A more sensitive parameter to monitor is the relative phase  $\varphi_{\text{rel}}$  between the rf oscillation and the spin precession. Assuming an initial phase  $\varphi_s$ , the free spin precession can be described by

$$\varphi = (2\pi\nu_s n + \varphi_s) \bmod 2\pi, \quad (8)$$

and, with the rf spin rotator operated at resonance,

$$\varphi_{\text{rel}} = \varphi_s - \varphi_{\text{rf}} \equiv \text{const.} \quad (9)$$

A frequency mismatch caused by variations of  $f_s$  and/or  $f_{\text{rf}}$  results in a varying relative phase

$$\frac{d\varphi_{\text{rel}}}{dt} = 2\pi(\Delta f_s - \Delta f_{\text{rf}}). \quad (10)$$

If one considers a possible frequency change corresponding to a spin tune change of  $\Delta\nu_s = 10^{-8}$ , this would correspond to a phase change of  $\Delta\varphi_{\text{rel}}$  close to  $2\pi$  over a typical cycle length of  $T = 100 \text{ s}$  (Figure 6 shows a measurement of the phase walk over a full cycle.). Thus, to summarize, for the presented case permanent monitoring and control of frequency and relative phase is mandatory.

### III. EXPERIMENTAL SETUP

All measurements were conducted at the Cooler Synchrotron COSY at the Forschungszentrum Jülich [13, 14]. The relevant beam parameters are listed in Table II. The implementation of the feedback system presented here is based on the following concept. Part of the COSY beam is used to permanently monitor the beam polarization by means of the analyzing power of elastic scattering on carbon. For this, the rates of particles scattered up, down, left, and right are recorded and the asymmetries are analyzed. Spin tune (*i.e.* spin precession frequency) and spin tune phase are determined as discussed in Ref. [10]. The stability of this phase w.r.t. the rf signal from the frequency generator of the Wien filter is continuously monitored and the latter is adjusted if needed.

A typical accelerator cycle proceeds as follows: A vector-polarized deuteron beam with its initial polarization perpendicular to the ring plane is injected and accelerated to a momentum of  $p = 970 \text{ MeV}/c$ . Throughout the cycle, a radio frequency cavity is used to bunch the beam. After the acceleration, the beam is electron-cooled in order to reduce its emittance. A final orbit correction

TABLE I. Overview of frequently used variables and parameters.

Description	Symbol	Defined in or near
Time in cycle	$t$	
Turn number	$n$	
Spin rotation angle per pass through an rf device	$\chi(t)$	Eq. (2)
Initial phase of the rf device	$\varphi_{\text{rf}}$	Eq. (2)
Invariant spin axis (unit vector)	$\vec{c}$	Fig. 2
Spin rotation axis of an rf device (unit vector)	$\vec{m}$	Fig. 2
Angle between the spin rotation axis $\vec{m}$ and the invariant spin axis $\vec{c}$	$\xi$	Eq. (4) and Fig. 2
Vertical polarization component	$p_v$	Eq. (4)
Oscillation frequency of the vertical spin component	$f_v$	Eq. (4)
Resonance strength	$\epsilon$	Eq. (4)
Out-of-plane angle of the polarization vector	$\alpha$	Eq. (21)
Spin precession phase	$\varphi$	Eq. (8)
Offset of the spin precession phase	$\varphi_s$	Eq. (8) and Eq. (11)
Relative phase between the spin tune and the rf Wien filter oscillation	$\varphi_{\text{rel}}$	Eq. (9)
Measured rf Wien filter phase	$\varphi_{\text{rf}}^{\text{meas}}$	Eq. (14)
Measured relative phase	$\varphi_{\text{rel}}^{\text{meas}}$	Eq. (15)
Demand relative phase	$\varphi_{\text{rel}}^{\text{demand}}$	Eq. (16)
Difference of the relative phase with respect to the demand value	$\Delta\varphi$	Eq. (16)
Averaged difference between the measured relative phase and the demand phase	$\Delta\varphi_{\text{avg}}$	Eq. (17)
Slope of the difference between the measured relative phase and the demand phase	$m$	Eq. (17)
Phase offset due to cable delays and latencies during signal processing	$\varphi_{\text{off}}$	Eq. (37)

TABLE II. Overview of frequently used beam parameters.

Description	Symbol	Value	Defined in or near
Beam revolution frequency	$f_{\text{rev}}$	750 kHz	Eq. (1)
Spin precession frequency	$f_s$	120 kHz	Eq. (1)
Lorentz factor	$\gamma$	1.126	Eq. (1)
Gyromagnetic anomaly	$G$	-0.143	Eq. (1)
Spin tune	$\nu_s$	-0.16	Eq. (1)
Frequency of the rf device	$f_{\text{rf}}$	871 kHz	Eq. (1) and Eq. (2)
Deuteron beam momentum	$p$	970 MeV/c	Section III

is then applied to have the beam running through the center of all elements. In a final step, the initial vertical polarization is rotated into the ring plane using an rf solenoid. It should be noted that this rotation occurs in less than a second and that the strength of the solenoid is large enough that an active control of the resonance frequency isn't necessary during this step. During beam preparation this setup is used to optimize the in-plane polarization lifetime (or spin-coherence time) by means of sextupoles as discussed in [15]. During the regular measurement the remaining part of the cycle is used to operate the rf Wien filter at resonance and a given relative phase  $\varphi_{\text{rel}}$  to determine the resonance strength  $\epsilon$ .

A sketch of the overall scheme of the active feedback system is depicted in Fig.3. For the measurements described in this paper, the WASA Forward Detector[16] and the Jedi Polarimeter (JePo) have been used, the latter specifically designed for EDM measurements[17]. During the measurements, the beam is continuously extracted onto an internal carbon target by applying a white noise excitation in a frequency band around a betatron resonance. Elastically scattered deuterons are detected by detector elements in four quadrants (up, down,

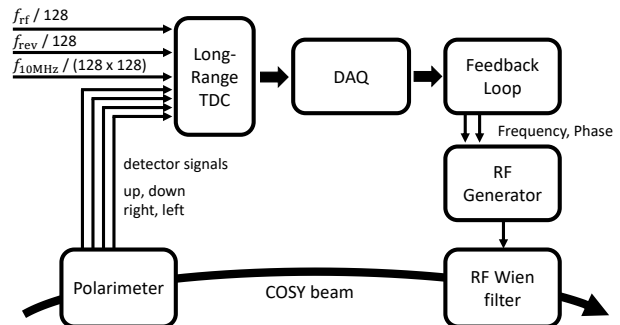


FIG. 3. Sketch of the experimental setup. The signals of the four detector quadrants as well as the pre-scaled frequency signals are fed into a long-range TDC, *i.e.* the same time reference was used for all signals. A 10 MHz reference signal is used for normalization. The DAQ system sends the time stamps into the feedback system, which then adjusts the frequency and phase of the rf generator of the Wien filter.

left, and right) around the beam pipe. The asymmetry of the measured rates in the left-right direction provides insight into the vertical component of the polarization, whereas the asymmetry in the up-down direction is a measure of the oscillating, radial in-plane component. Cycles with unpolarized beam are used to adjust any fake asymmetries from asymmetric detector acceptances. The frequency signals  $f_{\text{rf}}$ ,  $f_{\text{rev}}$  and  $f_{10\text{MHz}}$  from the rf Wien filter, the COSY rf cavity and the 10-MHz reference, respectively, are prescaled and received via an optical-fibre distribution system.

For data acquisition components developed for the

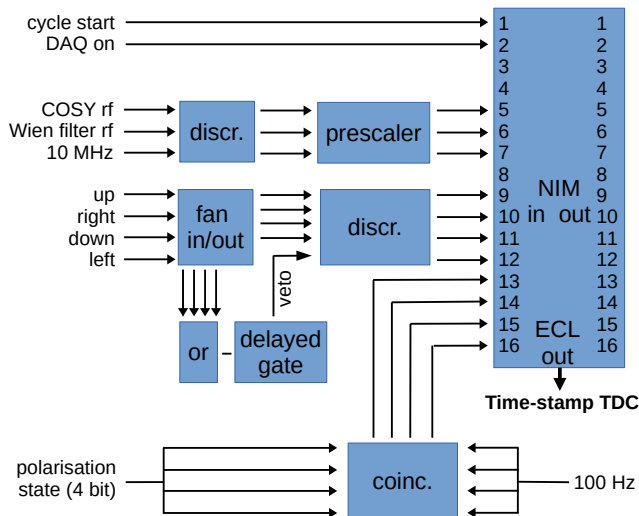


FIG. 4. Sketch of the main signal processing. All signals (control signals, frequencies, rates and polarization information) are fed into a single time-stamping TDC.

WASA detector based on a proprietary optimized back-plane bus with LVDS (Low Voltage Differential Signaling) technology [18] are used. The crates are equipped with a SIS1100/SIS3100 crate controller, the link to the readout computer is based on the physical layer of Gigabit Ethernet. The communication between readout computers and the phase-lock feedback system is done via TCP/IP over Gigabit Ethernet. As long-range Time-to-Digital Converter (TDC) a GPX-based model is used. The adjustable clock time period is set to 95.59 ps based on a single internal clock. For normalization an external, GPS-based reference signal of 10 MHz is used. The internal clock counter reaches its maximum value at 6.4  $\mu$ s, at which point an overflow bit is sent to a 20-bit register, allowing a full range up to approximately 6.7 s. During decoding, another overflow register is introduced, enabling continuous time-stamping of the registered events over the full measurement cycle.

The frequency and phase computed by the feedback system are communicated via Ethernet to the frequency generator (Rohde & Schwarz SMB100A) attached to the rf Wien filter. It is important to note, that this generator ensures a continuous phase evolution at a frequency change, *i.e.* no phase jumps. The frequency generator is operational at all times, allowing for the synchronization of its frequency and phase settings to the spin precession frequency while the rf Wien filter itself is deactivated. Once all preparations have been completed, the amplifiers of the Wien filter are activated, initiating the actual measurement process.

Figure 4 shows the processing of the main signals before entering the time-stamp TDC. The frequency signals are discriminated and prescaled by 128 (revolution frequency and Wien filter frequency) and  $128 \times 128$  (10

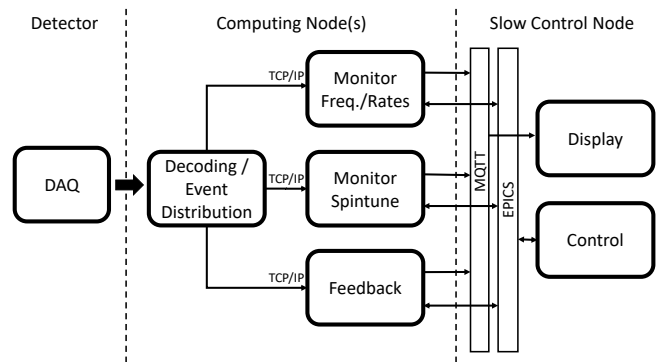


FIG. 5. Overall data processing scheme. The event stream from the Data Acquisition is distributed to multiple data processing routines, which uses MQTT and EPICS for communication.

MHz reference signal). A logical OR of the polarimeter signals is used to filter out signal bursts by applying a (typically 1  $\mu$ s long) veto signal keeping the rate within the specifications of the TDC. The information on the initial polarization state is provided via a 4-bit signal triggered with a 100 Hz clock. In addition, other slow control signals (cycle start as time reference, DAQ on) are monitored.

#### IV. THE PHASE-LOCK FEEDBACK

The phase-lock loop is implemented as part of a software package developed for monitoring all frequencies, rates, and asymmetries, as well as the spin tune and spin precession phase. A schematic is shown in Fig. 5. The data from the DAQ system are decoded and distributed to several processes. Each of these processes analyzes the data with respect to specific questions. This analysis is done in certain adjustable time intervals  $\Delta t$  (typically one second) and the results are sent to a slow control node for display via MQTT (Message Queuing Telemetry Transport, [19])<sup>1</sup> and also distributed and archived via EPICS (Experimental Physics and Industrial Control System, [20])<sup>2</sup>. The latter is also used to set all process parameters. In the case of more than one bunch in the ring, the system can be configured to monitor each bunch separately.

The main three processes are:

*a. Monitoring Rates and Frequencies* This process analyzes the frequencies, their stability, the detector rates, and the left/right asymmetry as a measure of the vertical polarization. In addition, the detector signals are

<sup>1</sup> See also: MQTT – The Standard for IoT Messaging, <https://mqtt.org>.

<sup>2</sup> See also: EPICS – Experimental Physics and Industrial Control System, <https://epics.anl.gov>.

plotted relative to the start of a  $f_{\text{rev}}$  oscillation period, reflecting the particle distribution in the ring and to unfold the longitudinal bunch extension in the processes b) and c).

*b. Spin Tune Monitoring* This process analyzes the up/down asymmetry as well as the spin tune and its phase as described in Ref. [10].

*c. Feedback* This process does the actual phase-lock feedback and is discussed below.

In each cycle, the measurement with the rf Wien filter was structured as follows:

1. Adjusting the Wien-filter frequency to the resonance frequency  $f_{\text{rf}} = |\nu_s - 1|f_{\text{rev}}$  (*i.e.*  $h = -1$ ), while the Wien filter power supplies are still off
2. Measuring the relative phase  $\varphi_{\text{rel}}$  between the generated Wien filter frequency and the spin precession
3. Correcting  $f_{\text{rf}}$  if needed and adjusting  $\varphi_{\text{rel}}$  by means of  $\varphi_{\text{rf}}$  to the demand value
4. Switching on the rf Wien filter power supplies
5. Maintaining  $\varphi_{\text{rel}}$  throughout the measurement by adjusting  $f_{\text{rf}}$  and  $\varphi_{\text{rf}}$
6. Switching off the rf Wien filter power supplies

The value for  $\nu_s$  used for calculating the initial value of  $f_{\text{rf}}$  is the averaged, high-precision spin tune  $\nu_s^{\text{fixed}}$  determined in the previous cycle[10]. The revolution frequency  $f_{\text{rev}}$  is fixed and defined in the accelerator control system.

The fixed spin tune  $\nu_s^{\text{fixed}}$  is also used to derive the actual spin tune — and, thus, the resonance frequency — from the phase walk relative to this assumed spin tune in the current cycle. As discussed in [10] this phase analysis is more sensitive and also faster than a direct bin-by-bin Fourier transform. In the following, the procedure is shortly summarized:

For every event, the spin-tune phase based on the assumed, fixed spin tune is calculated and mapped to a  $4\pi$  interval, *i.e.* two full precessions:

$$\varphi_i = (2\pi\nu_s^{\text{fixed}}n) \bmod 4\pi. \quad (11)$$

These values are accumulated in a histogram such, that events from the up and down detector elements are filled with the weight 1 and  $-1$ , respectively. Thus, the plot shows an asymmetry distribution as a function of the spin direction given by the spin precession phase: an unpolarized, constant background with a sinusoidal oscillation on top. The histogram is then normalized by the number of events to get an asymmetry range between -1 and 1. In order to remove the unpolarized background, the two half intervals of the second oscillation are interchanged and subtracted from the first one. What remains is a sinusoidal oscillation around zero as a function of  $\varphi \in [0, 2\pi)$  as shown in Fig. 6 (upper panel). This data is fitted according to

$$f(\varphi) = A \sin(\varphi + \varphi_s) \quad (12)$$

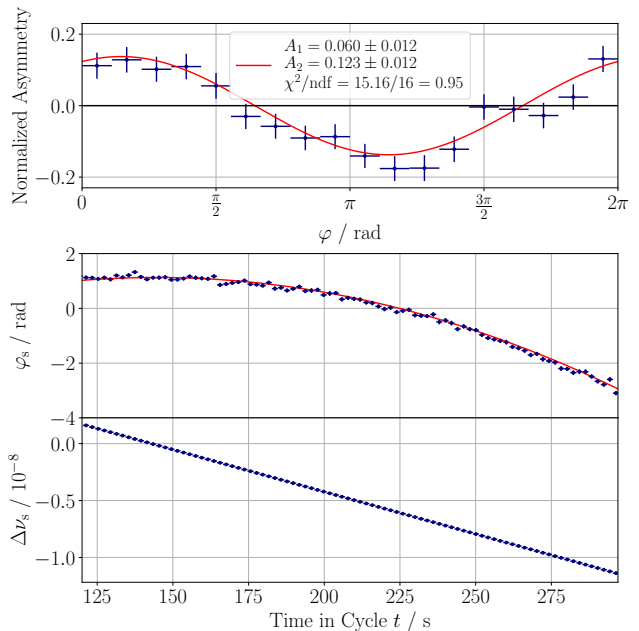


FIG. 6. Upper Panel: Normalized asymmetry as a function of the spin-tune phase based on the assumed, fixed spin tune (here  $\nu_s^{\text{fixed}} = 0.161\,006\,673\,7$ ) of data taken during a  $\Delta t = 1$  s period. The distribution is fitted according to Eq. (12). In this example the offset of the spin precession phase is  $\varphi_s = 1.12(8)$  rad. Lower Panels: Spin-tune phase offset and change of spin tune (according to Eq. (13), including uncertainties) as a function of time in the cycle. In this example, the change of the spin tune amounts to  $\Delta\nu_s \approx 10^{-8}$  during a 150 s interval.

with the spin-tune phase offset  $\varphi_s$  as fit parameter. (In practice, the fit formula is converted into its linear form  $a_1 \sin \varphi + a_2 \cos \varphi$ .)

It should be noted, that determining the phase  $\varphi_i$  assuming the spin tune  $\nu_s^{\text{fixed}}$ , which is slightly different to the real value, also means that the phase offset varies slightly within the measurement interval  $\Delta t$ . For typical operation parameters, the deviation from the fixed spin tune is within  $10^{-8}$ , corresponding to a phase change of less than 50 mrad per second. Thus, within the typical time interval of  $\Delta t = 1$  s,  $\varphi_s$  can be considered constant within each time bin and the distribution is mostly smeared by the longitudinal distribution of the bunch (typically  $\approx 500$  mrad). By extrapolating the change of the spin-tune phase offset, the change of spin tune during the cycle can be calculated using

$$\nu_s(t) = \nu_s^{\text{fixed}} + \frac{1}{2\pi f_{\text{rev}}} \frac{d\varphi_s}{dt} = \nu_s^{\text{fixed}} + \Delta\nu_s. \quad (13)$$

An example is shown in Fig. 6 (lower panel).

For the rf Wien filter, the current event time from the polarimeter is used to calculate the phase that the Wien filter frequency signal had at the time  $t_i$  of that event

$$\varphi_{\text{rf},i} = [2\pi \cdot (t_i - t_{\text{LastRfTag}}) \cdot f_{\text{rf}}] \bmod 2\pi. \quad (14)$$

Here,  $t_{\text{LastRfTag}}$  is the time stamp of the last zero crossing from negative to positive of the rf signal. In order to use  $\nu_s^{\text{fixed}}$  as reference, the difference between  $\varphi_i$  and  $\varphi_{\text{rf},i}$  is histogrammed. If sufficiently close to resonance, this difference can be considered constant. Finally, the event time relative to  $f_{\text{rev}}$  is used to approximately correct for the bunch width to get a more distinct signal. At the end of each time bin, the mean of the distribution is calculated as  $\varphi_{\text{rf}}^{\text{meas}}$ .

Then the relative phase is the difference between both:

$$\varphi_{\text{rel}}^{\text{meas}} = \varphi_s - \varphi_{\text{rf}}^{\text{meas}}. \quad (15)$$

Once the Wien filter frequency is set to its initial value at the beginning of the measurement cycle, the difference of the relative phase with respect to the demand value

$$\Delta\varphi = \varphi_{\text{rel}}^{\text{meas}} - \varphi_{\text{rel}}^{\text{demand}} \quad (16)$$

is continuously monitored according to the following scheme:

A sequence length  $N$  (typically 5-7) is defined via a control parameter and  $N$  subsequent values of  $\varphi_{\text{rel}}^{\text{meas}}$ , each within a time bin  $\Delta t$ , are recorded. After the last interval, these values are used to apply a linear fit

$$\Delta\varphi(j) = m \cdot \left( j - \frac{N-1}{2} \right) + \Delta\varphi_{\text{avg}} \quad (17)$$

with the bin number  $j \in [0, N-1]$ . As fit result, one gets the slope  $m$  and the average offset  $\Delta\varphi_{\text{avg}}$  together with the corresponding statistical uncertainties. In addition, the phase difference is extrapolated to bin number  $N$ , which is the first bin following the measurement sequence. This bin represents the interval during which the calculation and correction occur

$$\Delta\varphi(N) = \Delta\varphi_{\text{avg}} + m \cdot \frac{N+1}{2}. \quad (18)$$

Both the slope  $m$  and the offset of the phase difference,  $\Delta\varphi_{\text{avg}}$  or  $\Delta\varphi(N)$ , are considered "good" if their deviations from zero fall within two standard deviations. When this condition is met, no correction is applied, otherwise frequency and/or phase are corrected accordingly:

$$f_{\text{rf}} \rightarrow f_{\text{rf}} - \frac{1}{2\pi\Delta t} m, \quad (19)$$

$$\varphi_{\text{rf}} \rightarrow \varphi_{\text{rf}} - \Delta\varphi_{\text{rf}}, \quad (20)$$

with  $\Delta\varphi_{\text{rf}}$  either  $\Delta\varphi_{\text{avg}}$  or  $\Delta\varphi(N)$ . For the slope  $m$  the statistical error from the fit is used, for the phase several approaches were considered:

- Using the average phase difference  $\Delta\varphi_{\text{avg}}$  as  $\Delta\varphi_{\text{rf}}$  and its statistical error in cases without frequency correction, and using the extrapolated phase value  $\Delta\varphi(N)$  when a frequency correction is applied. Alternatively,  $\Delta\varphi(N)$  could be used in all cases, regardless of a frequency correction.

- For the uncertainty of  $\Delta\varphi(N)$ , either using the uncertainty of  $\Delta\varphi_{\text{avg}}$  directly or propagating the uncertainty of the slope  $m$  in addition.

For standard data taking, the option to use  $\Delta\varphi(N)$  together with the uncertainty of the averaged phase has been selected and is presented here.

As all corrections are applied during interval  $N$ , this bin and the next one are skipped and the collection of samples continues at interval  $N+2$ .

Fig. 7 illustrates the procedure. For two different cycles, several measurement blocks with 7+2 measurement bins are shown together with the fits to the data and the correction to phase and frequency. The resulting distributions of  $\Delta\varphi$  have a typical width of  $\sigma_{\Delta\varphi} \approx 0.2$  rad. This is consistent with the value reported for the first commissioning run, when the revolution frequency was controlled [7].

Depending on the variation of the spin tune in the cycle (see Fig. 6), the average relative phase shows a systematic deviation from the demand value. Therefore, in the data analysis, the measured relative phase has to be used rather than the demand one.

There are certain limitations and caveats that need to be mentioned:

1. The spin tune and its phase are determined from the oscillating radial in-plane polarization. For the analysis, the measured in-plane polarization  $p_h$  has to be non-zero taking into account its uncertainty. Hence, the feedback stops working when either the polarization itself becomes too small or the direction of the polarization vector approaches the vertical direction.
2. The measured relative phase  $\varphi_{\text{rel}}$  differs from the true value in the rf spin rotator due to several factors. These include cable delays and latencies, as well as the additional spin precession that occurs between the positions of the rf spin rotator and the detector. In multi-bunch setups, offsets between the bunches result from the different spin orientations determined by the selection of harmonics and from corrections to account for the particle distribution in the ring. While these offsets remain constant for a given setup and the feedback system provides a stabilization of the relative phase, the real phase must be extracted from the data when needed.
3. Spin oscillations show a certain phase walk compared to the free, in-plan precession (see Ref. [11] and Fig. 5 and 6 therein). Thus, when the phase-lock feedback system is operated on the same bunch, which is also affected by the rf spin rotator, this phase walk is disturbed and the observed signal is modified. However, this can also be taken into account as discussed in the next section.

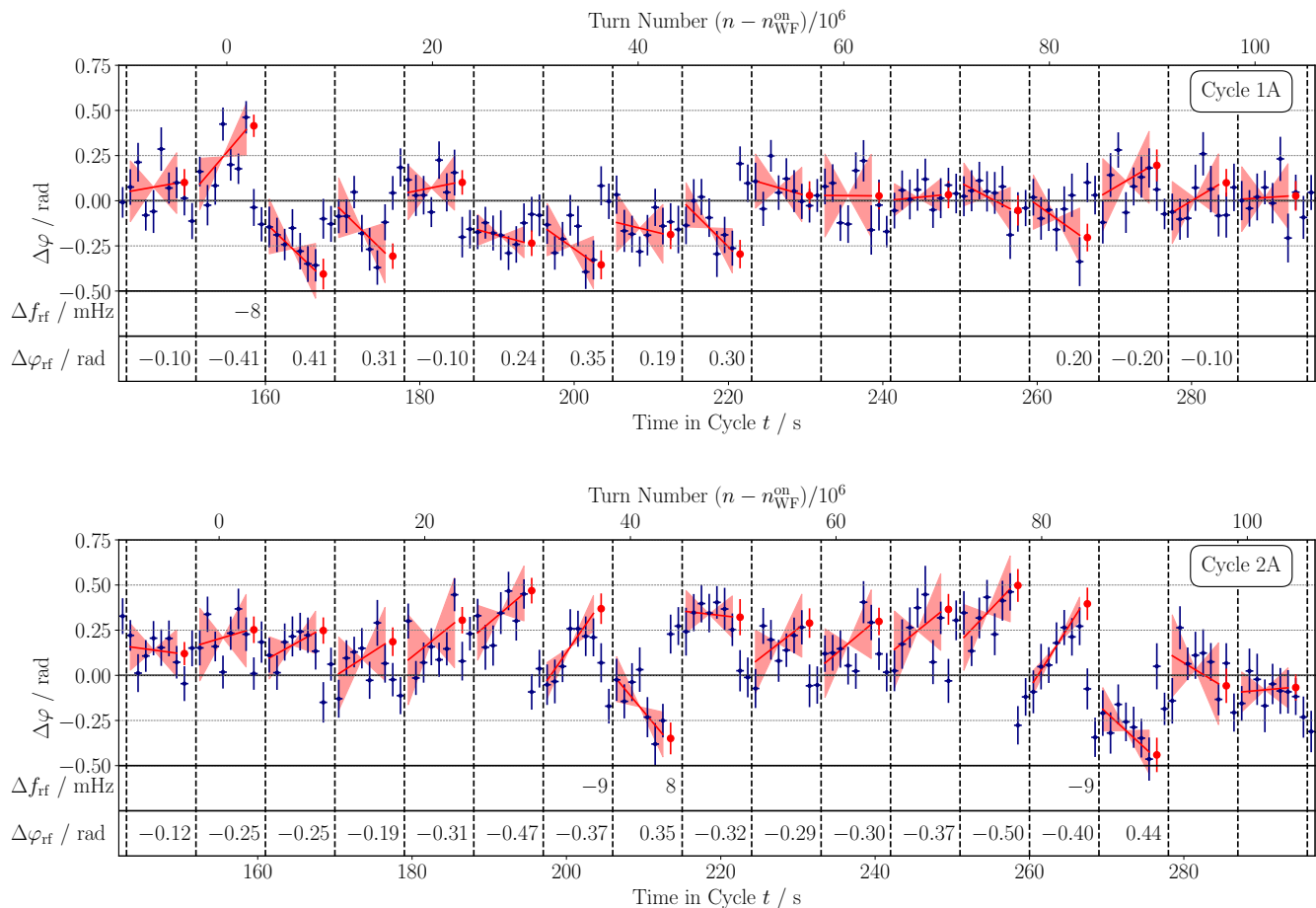


FIG. 7. Frequency and phase corrections derived from the measured relative phase for two exemplary cycles labeled 1A and 2A. The upper panel in each plot shows the difference of the relative phase with respect to the demand value  $\Delta\varphi$  as a function of the time in cycle. The time axis is divided in several blocks with 7+2 measurement bins each ( $\Delta t = 1$  s) indicated by dashed lines. The first 7 values in each block are fitted linearly followed by a correction of frequency and/or phase shown below if the deviation is significant as defined in the text. The red dots show the extrapolated values for the phase difference, the red lines the fitted slope. The error bars and the shaded area indicate the allowed  $2\sigma$  range for phase offset and slope. While the applied corrections are indicated only at the time of correction, all changes are additive. The corresponding distributions of  $\Delta\varphi$  have a width of  $\sigma_{\Delta\varphi} = 0.16$  rad and  $\sigma_{\Delta\varphi} = 0.21$  rad centered at  $\Delta\varphi = -0.04$  rad and  $\Delta\varphi = 0.10$  rad, respectively.

## V. EFFECT OF THE PHASE-LOCKING ON THE SPIN ROTATIONS IN THE WIEN FILTER

The effect mentioned above, that an rf spin rotator normally modifies the spin precession phase while rotating the spin also means that an active phase-lock has an impact on the primary observable, the vertical spin oscillation. In Ref. [11] the phase walk while applying a rf solenoid as spin rotator has been measured and discussed in detail, on resonance as well as off resonance. There the feedback system has only been used to define the starting condition (the initial relative phase). The results have been described by a set of differential equations for the out-of-plane angle  $\alpha$  of the spin direction and the relative phase  $\varphi_{rel}$ . Although these equations were developed under the assumption of an ideal ring, *i.e.* neglecting spin

decoherence and other systematic effects, the data could be fitted quite well. They are also used here to illustrate the two scenarios, in which the feedback has been operated, especially because the difference in the resulting phase relations can be easily implemented by modifying a single equation. Although cycles with long spin coherence times have been chosen to minimize systematic effects in the presented data, the corresponding  $\chi^2$  values indicate their presence. All cited uncertainties are statistical only and should be interpreted accordingly. For the final analysis of the EDM data a more sophisticated and complete model incorporating these effects is used [21].

The two equations from Ref. [11] are

$$\frac{d\alpha}{dn} = \frac{k}{2} \cos \varphi_{rel} \quad (21)$$

$$\frac{d\varphi_{\text{rel}}}{dn} = \frac{k}{2} (\sin \varphi_{\text{rel}} \tan \alpha + q) \quad (22)$$

and the relation to the variables defined in this paper is given by

$$k = -\chi_0 \sin \xi = -4\pi\epsilon \quad (23)$$

$$q = \frac{4\pi\Delta f}{kf_{\text{rev}}} \quad (24)$$

with  $k$  defining the strength of the rf device and  $q$  being the off-resonance parameter.

There is also an analytic solution given:

$$p_y(n) = \sin \alpha(n) = A_1 \sin(A_2 + A_3 n) - A_4, \quad (25)$$

$$\cos \varphi_{\text{rel}}(n) = \frac{A_1 \sqrt{1+q^2} \cos(A_2 + A_3 n)}{\sqrt{1 - (A_1 \sin(A_2 + A_3 n) - A_4)^2}}, \quad (26)$$

$$\sin \varphi_{\text{rel}}(n) = \frac{C + q \sin \alpha(n)}{\cos \alpha(n)}, \quad (27)$$

with the parameters

$$A_1 = \frac{\sqrt{1+q^2 - C^2}}{1+q^2}, \quad (28)$$

$$A_2 = \begin{cases} \arcsin\left(\frac{\sin \alpha(0) + A_4}{A_1}\right) & |\varphi_{\text{rel}}(0)| < \pi/2, \\ \pi - \arcsin\left(\frac{\sin \alpha(0) + A_4}{A_1}\right) & |\varphi_{\text{rel}}(0)| > \pi/2, \end{cases} \quad (29)$$

$$A_3 = \frac{k}{2} \sqrt{1+q^2}, \quad (30)$$

$$A_4 = \frac{Cq}{1+q^2}, \quad (31)$$

$$C = \cos \alpha \sin \varphi_{\text{rel}} - q \sin \alpha = \text{const.} \quad (32)$$

The starting conditions at the time the Wien filter is switched on are given by  $\alpha(0)$  and  $\varphi_{\text{rel}}(0)$ .  $A_1$  is the oscillation amplitude,  $A_2$  is the phase offset of the oscillation matching the start conditions,  $A_3$  is the oscillation frequency and  $A_4$  is the central value of the oscillation, which is shifted when being off-resonance.  $C$  is an auxiliary variable defined by Eq. 27. In the following, these equations are used to discuss certain properties of the system.

It should be noted that the definition of  $\varphi_{\text{rel}} = 0$  here differs from the one used as experimental observable in Sect. IV. The measured spin-tune phase based on the up-down asymmetry in the polarimeter is relative to the beam direction.  $\varphi_{\text{rel}}$  here is 0 when the projection of the polarization vector into the plane perpendicular to the invariant spin axis  $\vec{c}$  is parallel to  $\vec{c} \times \vec{m}$  when the field in the rf spin rotator is at maximum. This adds another contribution to the setup-specific offset  $\varphi_{\text{off}}$ , but has no effect on the following discussion.

TABLE III. Fit parameters from Fig. 8

	Cycle 1B	Cycle 2B
$\varphi_{\text{rel}}^{\text{demand}} / \text{rad}$	2.36	5.50
$\varphi_{\text{rel}}^{\text{meas}} / \text{rad}$	2.29(1)	5.43(1)
$\sigma_{\Delta\varphi_{\text{rel}}} / \text{rad}$	0.27	0.18
$d\alpha/dt / \text{rad/s}$	-0.020(7)	0.0186(6)
$\alpha(0) / \text{rad}$	-0.04(2)	-0.06(2)
$\chi^2/\text{ndf}$	51/57	61/60

### A. Resonance Width

As mentioned before, the necessity to control the generator frequency  $f_{\text{rf}}$  can be judged using the resonance width  $\Gamma$  of the rf spin rotator. Thus, one needs a proper estimate for  $\Gamma$ . One can utilize the parameter  $A_1$  from Eq. (28), which quantifies the oscillation amplitude. When starting with the spin along the invariant spin axis ( $\alpha(0) = \pi/2$  and any  $\varphi_{\text{rel}}(0)$ ), the parameter  $C$  amounts to  $q^2$  and with Eq. (24)  $A_1$  can be written in the same analytic form as a Lorentz function:

$$A_1 = \frac{1}{1+q^2} = \frac{(\Gamma/2)^2}{(\Gamma/2)^2 + (\Delta f)^2} \quad (33)$$

with  $\Gamma = kf_{\text{rev}}/2\pi = 2\epsilon f_{\text{rev}}$ . This can be used as a first criterion whether an active control loop is needed or not.

### B. Phase Locking with a Single Bunch

As discussed in Ref. [11] and indicated by Eq. 22 the relative phase  $\varphi_{\text{rel}}$  is changing during an rf-induced spin oscillation. Frequency synchronisation with phase locking prevents these changes. Considering this effect is straight forward by replacing Eq. (22) with

$$\frac{d\varphi_{\text{rel}}}{dn} = 0. \quad (34)$$

The remaining Eq. (21) with a now constant phase  $\varphi_{\text{rel}} = \varphi_{\text{rel}}(0)$  describes a linear increase in  $\alpha$  with a phase dependent slope:

$$\frac{d\alpha}{dt} = 2\pi\epsilon f_{\text{rev}} \cos \varphi_{\text{rel}}. \quad (35)$$

This results in a spin oscillation of the form

$$p_y(t) = \sin(\cos \varphi_{\text{rel}} \cdot 2\pi\epsilon f_{\text{rev}} t). \quad (36)$$

The oscillation amplitude is always 1 (*i.e.* the spin is fully rotated into the vertical direction independent of the relative phase) and the oscillation frequency is modulated by the phase. As a direct implication, this method can only be used for less than a quarter of a full oscillation, because the feedback stops working when the in-plane component vanishes.

Fig. 8 shows data for two different relative phases. The slope is linear until the feedback stops working and the

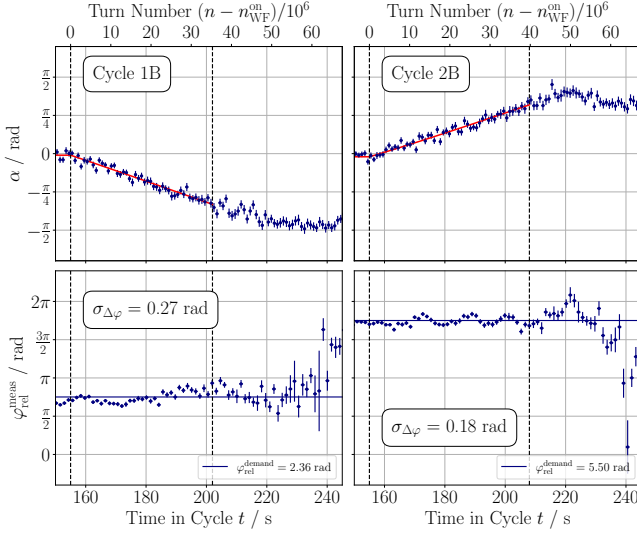


FIG. 8. With phase locking: Out-of-plane angle  $\alpha$  and relative phase  $\varphi_{\text{rel}}$  as a function of time for two different initial values of  $\varphi_0$  labeled as cycles 1B and 2B. The first dashed line marks  $t_{\text{WF}}^{\text{on}}$ . The second dashed line marks the timestamp at which the phase feedback is switched off. For the fit parameters see Table III.

phase is no longer stabilized. The fit results are summarized in Table III.

With this method, the resonance strength  $\epsilon$  can be extracted by varying  $\varphi_{\text{rel}}$  from cycle to cycle and fitting the sinusoidal dependence of the slope  $\dot{\alpha}$ . This is shown in Fig. 9. The data are fitted using Eq. (35) using

$$\varphi_{\text{rel}}^{\text{meas}} = \varphi_{\text{rel}} + \varphi_{\text{off}} \quad (37)$$

introducing the additional parameter  $\varphi_{\text{off}}$  to address the unknown, but constant setup-specific offset. Considering the result of  $\varphi_{\text{off}} = -1.335$  rad for this particular fit, the values for  $\varphi_{\text{rel}}$  for the exemplary cycles in Fig. 8 are  $\varphi_{\text{rel}}^{1\text{B}} = 3.65$  rad and  $\varphi_{\text{rel}}^{2\text{B}} = 0.51$  rad, *i.e.* close to the optimal phases of 0 and  $\pi$ .

### C. Phase Locking with Two Bunches

Stabilizing the relative phase and, at the same time, allowing an rf-induced change of  $\varphi_{\text{rel}}$  is only possible using a second bunch, which is kept undisturbed by the rf spin rotator. This was achieved in the second run in 2021, when two bunches were used and the Wien filter was disabled for the second bunch by means of fast switches [8].

For such a resonant operation ( $q = 0$ ) starting with the spin precessing in the ring plane ( $\alpha(0) = 0$ ) one can simplify the equations (28)–(31):

$$A_1 = |\cos \varphi_{\text{rel}}(0)| \quad (38)$$

$$A_2 = 0 \text{ or } \pi \quad (39)$$

$$A_3 = k/2 \quad (40)$$

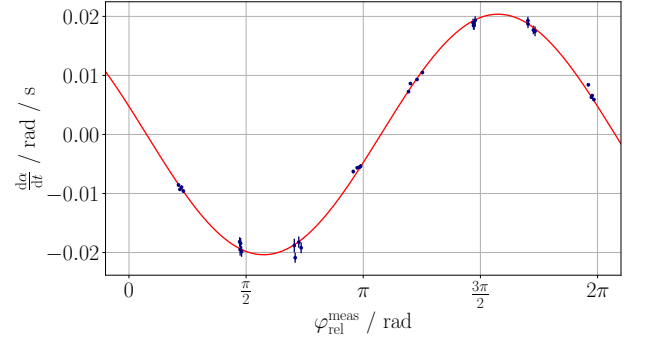


FIG. 9. Sinusoidal dependence of the initial slope as a function of the relative phase for the phase-locked case as shown in Fig. 8. The fit parameters according to Eqs. (35) and (37) are given by  $\epsilon = 4.32(3) \times 10^{-9}$ ,  $\varphi_{\text{off}} = -1.335(5)$  rad, and  $\chi^2/\text{ndf} = 55.13/30 = 1.83$ .

TABLE IV. Fit parameters from Fig. 10

	Cycle 1A	Cycle 2A
<b>Unaffected bunch</b>		
$\varphi_{\text{rel}}^{\text{demand}} / \text{rad}$	0.90	4.50
$\varphi_{\text{rel}}^{\text{meas}} / \text{rad}$	0.86(1)	4.60(1)
$\sigma_{\Delta\varphi_{\text{rel}}} / \text{rad}$	0.16	0.21
<b>Signal bunch</b>		
$A_1$	0.968(2)	0.908(3)
$A_2$	$\pi + 0.07(1)$	0.00(1)
$A_3$	$6.38(2) \times 10^{-8}$	$6.49(3) \times 10^{-8}$
$A_4$	-0.017(3)	-0.029(4)
$C$	-0.73(2)	0.99(2)
$k$	$1.27(1) \times 10^{-7}$	$1.29(1) \times 10^{-7}$
$q$	-0.07(3)	-0.07(2)
$\alpha(0) / \text{rad}$	-0.05(3)	0.03(3)
$\varphi_{\text{rel}}^{\text{meas}}(0) / \text{rad}$	3.96(3)	1.42(1)
$\varphi_{\text{off}}$	1.07(1)	0.99(1)
$\varphi_{\text{rel}}(0) / \text{rad}$	2.89(3)	0.43(1)
$\chi^2/\text{ndf}$	370/277	496/277

$$A_4 = 0 \quad (41)$$

and obtains

$$p_y(n) = \sin \alpha(n) = \cos \varphi_{\text{rel}}(0) \sin(kn/2) \quad (42)$$

or

$$p_y(t) = \sin \alpha(t) = \cos \varphi_{\text{rel}}(0) \sin(2\pi\epsilon f_{\text{rev}}t). \quad (43)$$

This is consistent with the expectation: the amplitude of the oscillation depends on the initial relative phase  $\varphi_{\text{rel}}(0)$  and the oscillation frequency is fixed at  $\omega = 2\pi\epsilon f_{\text{rev}}$ , which can then be used to extract the resonance strength  $\epsilon$ .

The result of such a measurement is shown in Fig. 10. Here, the out-of-plane angle of the polarization vector and the relative phase are plotted versus the time in cycle for two different initial relative phases using the same

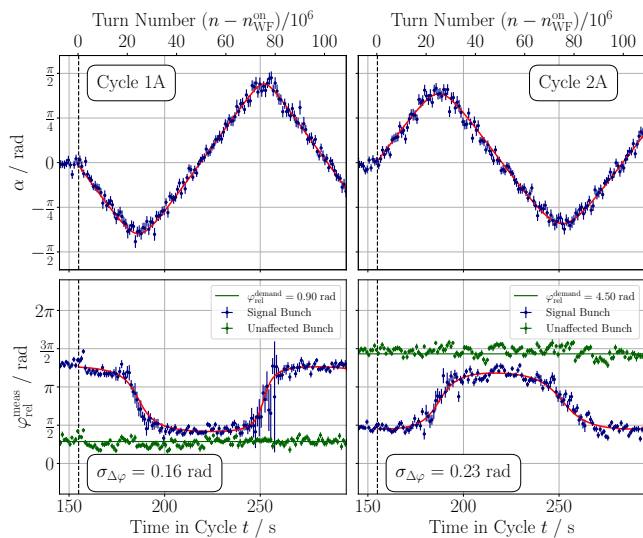


FIG. 10. Out-of-plane angle  $\alpha$  (top) and relative phase  $\varphi_{\text{rel}}^{\text{meas}}$  (bottom) as a function of time for two initial values of  $\varphi_{\text{rel}}^{\text{demand}}$  (left and right). The dashed line marks the time the Wien filter is switched on at  $t_{\text{WF}}^{\text{on}}$ . The blue data points represent the signal bunch, the green ones the unaffected bunch used by the feedback system. The fit parameters are listed in Table IV.

two cycles 1A and 2A, that are shown in Fig. 7. Each cycle is fitted with the general Eqs. (25)-(27) simultaneously. The green data points in the phase plot show the unaffected bunch, which is used to monitor and control frequency and phase. The blue data points show the signal bunch.

The corresponding fit results are shown in Table IV. In addition to the variables  $A_1$  to  $A_4$  and  $C$  also the values for  $k$ ,  $q$  and the start values  $\alpha(0)$  and  $\varphi_{\text{rel}}^{\text{meas}}(0)$  are listed. The values of  $A_1$  to  $A_4$  are close to the optimal ones in Eqs. (38)-(41) indicating the successful operation of the feedback system. The number for the off-resonance parameter  $q$  slightly differs from zero if only the statistical error is considered. However, as mentioned before the fit quality suggests additional systematic uncertainties and, thus, larger error margins. Furthermore, its value corresponds to a frequency deviation of  $|\Delta f| \approx 5 \times 10^{-4}$  Hz (see Eq. (24)), which has to be compared to the step size of the frequency generator of  $10^{-3}$  Hz.

In the fits, the offset parameter  $\varphi_{\text{off}}$  amounts to  $\approx 1$  rad for this setup. Thus, the actual relative phases for the signal bunch are  $\varphi_{\text{rel}}^{1A} \approx 2.9$  rad and  $\varphi_{\text{rel}}^{2A} \approx 0.4$  rad. These relative phases are close the optimal phases, but not exactly. Thus, the oscillation of the polarization vector does not reach the maximum out-of-plane angles of  $\pm\pi/2$  ( $A_1 = |\cos \varphi_{\text{rel}}(0)|$ ).

In general, there is a good agreement between the analytical model and the data presented in Figs. 8 and 10.

While the scenarios discussed in the last two subsec-

tions VB and VC result in a different evolution of the polarization vector, it should be noted, that the on-set when switching on the Wien filter remains the same in both cases: when comparing Eq. (35) with Eq. (43), one gets

$$\left. \frac{d\alpha}{dt} \right|_{t=0}^{\text{Eq.(35)}} = \left. \frac{d\alpha}{dt} \right|_{t=0}^{\text{Eq.(43)}} = 2\pi\epsilon f_{\text{rev}} \quad (44)$$

using the same experimental conditions. Concerning the numerical value of the initial slope, the results shown in Figs.8 and 10 are not directly comparable, because they were taken in two different beam times with two different setups (2018 and 2021), and both the Wien filter power and the setup changed.

## VI. SUMMARY & CONCLUSION

This paper describes the successful operation of a feedback system to maintain a resonance condition between a 120 kHz spin precession in a storage ring and a radio frequency device (Wien filter) operated at a harmonic of the spin precession. By measuring the spin precession, the frequency and phase of the Wien filter were adjusted in order to maintain a constant but selectable phase difference between the spin precession and the Wien filter. The successful operation of the phase-lock feedback can be quantified using the variation of the phase with respect to the demand phase, which is on average in the order of  $\sigma_{\Delta\varphi} \approx 0.2$  rad. The measured time dependence of the polarization vector and the relative phase is in good agreement with an analytical model.

Feedback systems of this type are mandatory for proposed storage ring experiments using polarized beam in order to search for example for electric dipole moments or axion/ALPs.

## VII. ACKNOWLEDGMENTS

We thank the COSY crew for their support in operating the COSY accelerator for the experiment. The work presented here has been carried out in the framework of the JEDI collaboration and was supported by an ERC Advanced Grant from the European Union (Proposal No. 694340: Search for electric dipole moments using storage rings). The work of A. Aksentev, A. Melnikov and N.N. Nikolaev was supported by the Russian Science Foundation (Grant No.22-42-04419). This research is part of a project funded by the European Union's Horizon 2020 research and innovation program under grant agreement STRONG-2020-No. 824093.

- [1] J. Slim, R. Gebel, D. Heberling, F. Hinder, D. Hölscher, A. Lehrach, B. Lorentz, S. Mey, A. Nass, F. Rathmann, L. Reifferscheidt, H. Soltner, H. Straatmann, F. Trinkel, and J. Wolters, *Electromagnetic Simulation and Design of a Novel Waveguide RF Wien Filter for Electric Dipole Moment Measurements of Protons and Deuterons*, *Nuclear Instruments and Methods in Physics Research Section A: Accelerators, Spectrometers, Detectors and Associated Equipment* **828**, 116 (2016).
- [2] J. Slim, A. Nass, F. Rathmann, H. Soltner, G. Tagliente, and D. Heberling, *The driving circuit of the waveguide RF Wien filter for the deuteron EDM precursor experiment at COSY*, *Journal of Instrumentation* **15** (03), P03021.
- [3] S. Navas *et al.* (Particle Data Group), *Review of particle physics*, *Phys. Rev. D* **110**, 030001 (2024).
- [4] F. Rathmann, A. Saleev, and N. N. Nikolaev, *The search for electric dipole moments of light ions in storage rings*, *Journal of Physics: Conference Series* **447**, 012011 (2013).
- [5] W. M. Morse, Y. F. Orlov, and Y. K. Semertzidis, *Rf Wien filter in an electric dipole moment storage ring: The “partially frozen spin” effect*, *Physical Review Special Topics - Accelerators and Beams* **16**, 114001 (2013).
- [6] F. Rathmann, N. N. Nikolaev, and J. Slim, *Spin dynamics investigations for the electric dipole moment experiment*, *Physical Review Accelerators and Beams* **23**, 024601 (2020).
- [7] N. Hempelmann, V. Hejny, J. Pretz, E. Stephenson, W. Augustyniak, Z. Bagdasarian, M. Bai, L. Barion, M. Berz, S. Chekmenev, G. Ciullo, S. Dymov, F.-J. Etzkorn, D. Eversmann, M. Gaisser, R. Gebel, K. Grigoryev, D. Grzonka, G. Guidoboni, T. Hanraths, D. Heberling, J. Hetzel, F. Hinder, A. Kacharava, V. Kamerdzhev, I. Keshelashvili, I. Koop, A. Kulikov, A. Lehrach, P. Lenisa, N. Lomidze, B. Lorentz, P. Maanen, G. Macharashvili, A. Magiera, D. Mchedlishvili, S. Mey, F. Müller, A. Nass, N. N. Nikolaev, A. Pesce, D. Prasuhn, F. Rathmann, M. Rosenthal, A. Saleev, V. Schmidt, Y. Semertzidis, V. Shmakova, A. Silenko, J. Slim, H. Soltner, A. Stahl, R. Stassen, H. Stockhorst, H. Ströher, M. Tabidze, G. Tagliente, R. Talman, P. Thörngren Engblom, F. Trinkel, Yu. Uzikov, Yu. Valdau, E. Valetov, A. Vassiliev, C. Weidemann, A. Wrońska, P. Wüstner, P. Zuprański, and M. Żurek, *Phase Locking the Spin Precession in a Storage Ring*, *Physical Review Letters* **119**, 014801 (2017).
- [8] J. Slim, F. Rathmann, A. Andres, V. Hejny, A. Nass, A. Kacharava, P. Lenisa, N. N. Nikolaev, J. Pretz, A. Saleev, V. Shmakova, H. Soltner, F. Abusaif, A. Aggarwal, A. Aksentev, B. Alberdi, L. Barion, I. Bekman, M. Beyß, C. Böhme, B. Breikreutz, N. Canale, G. Ciullo, S. Dymov, N.-O. Fröhlich, R. Gebel, M. Gaisser, K. Grigoryev, D. Grzonka, J. Hetzel, O. Javakhishvili, V. Kamerdzhev, S. Karanth, I. Keshelashvili, A. Kononov, K. Laihem, A. Lehrach, N. Lomidze, B. Lorentz, G. Macharashvili, A. Magiera, D. Mchedlishvili, A. Melnikov, F. Müller, A. Pesce, V. Poncza, D. Prasuhn, D. Shergelashvili, N. Shurkhno, S. Siddique, A. Silenko, S. Stassen, E. J. Stephenson, H. Ströher, M. Tabidze, G. Tagliente, Y. Valdau, M. Vitz, T. Wagner, A. Wirzba, A. Wrońska, P. Wüstner, and M. Żurek, *Pilot bunch and co-magnetometry of polarized particles stored in a ring* (2023), arXiv:2309.06561 [hep-ex, physics:physics].
- [9] Z. Bagdasarian, S. Bertelli, D. Chiladze, G. Ciullo, J. Dietrich, S. Dymov, D. Eversmann, G. Fanourakis, M. Gaisser, R. Gebel, B. Gou, G. Guidoboni, V. Hejny, A. Kacharava, V. Kamerdzhev, A. Lehrach, P. Lenisa, B. Lorentz, L. Magallanes, R. Maier, D. Mchedlishvili, W. M. Morse, A. Nass, D. Oellers, A. Pesce, D. Prasuhn, J. Pretz, F. Rathmann, V. Shmakova, Y. K. Semertzidis, E. J. Stephenson, H. Stockhorst, H. Ströher, R. Talman, P. Thörngren Engblom, Yu. Valdau, C. Weidemann, and P. Wüstner, *Measuring the polarization of a rapidly precessing deuteron beam*, *Physical Review Special Topics - Accelerators and Beams* **17**, 052803 (2014).
- [10] D. Eversmann, V. Hejny, F. Hinder, A. Kacharava, J. Pretz, F. Rathmann, M. Rosenthal, F. Trinkel, S. Andrianov, W. Augustyniak, Z. Bagdasarian, M. Bai, W. Bernreuther, S. Bertelli, M. Berz, J. Bsaisou, S. Chekmenev, D. Chiladze, G. Ciullo, M. Contalbrigo, J. de Vries, S. Dymov, R. Engels, F. M. Esser, O. Felden, M. Gaisser, R. Gebel, H. Glückler, F. Goldenbaum, K. Grigoryev, D. Grzonka, G. Guidoboni, C. Hanhart, D. Heberling, N. Hempelmann, J. Hetzel, R. Hipple, D. Hölscher, A. Ivanov, V. Kamerdzhev, B. Kamys, I. Keshelashvili, A. Khokkaz, I. Koop, H.-J. Krause, S. Krewald, A. Kulikov, A. Lehrach, P. Lenisa, N. Lomidze, B. Lorentz, P. Maanen, G. Macharashvili, A. Magiera, R. Maier, K. Makino, B. Mariański, D. Mchedlishvili, U.-G. Meißner, S. Mey, A. Nass, G. Natour, N. Nikolaev, M. Nioradze, A. Nogga, K. Nowakowski, A. Pesce, D. Prasuhn, J. Ritman, Z. Rudy, A. Saleev, Y. Semertzidis, Y. Senichev, V. Shmakova, A. Silenko, J. Slim, H. Soltner, A. Stahl, R. Stassen, M. Statera, E. Stephenson, H. Stockhorst, H. Straatmann, H. Ströher, M. Tabidze, R. Talman, P. Thörngren Engblom, A. Trzciński, Yu. Uzikov, Yu. Valdau, E. Valetov, A. Vassiliev, C. Weidemann, C. Wilkin, A. Wirzba, A. Wrońska, P. Wüstner, M. Zakrzewska, P. Zuprański, and D. Zyuzin, *New Method for a Continuous Determination of the Spin Tune in Storage Rings and Implications for Precision Experiments*, *Physical Review Letters* **115**, 094801 (2015).
- [11] N. Hempelmann, V. Hejny, J. Pretz, H. Soltner, W. Augustyniak, Z. Bagdasarian, M. Bai, L. Barion, M. Berz, S. Chekmenev, G. Ciullo, S. Dymov, D. Eversmann, M. Gaisser, R. Gebel, K. Grigoryev, D. Grzonka, G. Guidoboni, D. Heberling, J. Hetzel, F. Hinder, A. Kacharava, V. Kamerdzhev, I. Keshelashvili, I. Koop, A. Kulikov, A. Lehrach, P. Lenisa, N. Lomidze, B. Lorentz, P. Maanen, G. Macharashvili, A. Magiera, D. Mchedlishvili, S. Mey, F. Müller, A. Nass, N. N. Nikolaev, M. Nioradze, A. Pesce, D. Prasuhn, F. Rathmann, M. Rosenthal, A. Saleev, V. Schmidt, Y. Semertzidis, Y. Senichev, V. Shmakova, A. Silenko, J. Slim, A. Stahl, R. Stassen, E. Stephenson, H. Stockhorst, H. Ströher, M. Tabidze, G. Tagliente, R. Talman, P. Thörngren Engblom, F. Trinkel, Yu. Uzikov, Yu. Valdau, E. Valetov, A. Vassiliev, C. Weidemann, A. Wrońska, P. Wüstner, P. Zuprański, and M. Żurek, *Phase measurement for*

- driven spin oscillations in a storage ring, *Physical Review Accelerators and Beams* **21**, 042002 (2018).
- [12] A. Saleev, N. Nikolaev, F. Rathmann, W. Augustyniak, Z. Bagdasarian, M. Bai, L. Barion, M. Berz, S. Chekmenev, G. Ciullo, S. Dymov, D. Eversmann, M. Gaisser, R. Gebel, K. Grigoryev, D. Grzonka, G. Guidoboni, D. Heberling, V. Hejny, N. Hempelmann, J. Hetzel, F. Hinder, A. Kacharava, V. Kamerdzhev, I. Keshelashvili, I. Koop, A. Kulikov, A. Lehrach, P. Lenisa, N. Lomidze, B. Lorentz, P. Maanen, G. Macharashvili, A. Magiera, D. McHedlishvili, S. Mey, F. Müller, A. Nass, A. Pesce, D. Prasuhn, J. Pretz, M. Rosenthal, V. Schmidt, Y. Semertzidis, Y. Senichev, V. Shmakova, A. Silenko, J. Slim, H. Soltner, A. Stahl, R. Stassen, E. Stephenson, H. Stockhorst, H. Ströher, M. Tabidze, G. Tagliente, R. Talman, P. Engblom, F. Trinkel, Y. Uzikov, Y. Valdau, E. Valetov, A. Vassiliev, C. Weidemann, A. Wrońska, P. Wüstner, P. Zuprański, and M. Żurek, Spin tune mapping as a novel tool to probe the spin dynamics in storage rings, *Physical Review Accelerators and Beams* **20**, 10.1103/PhysRevAccelBeams.20.072801 (2017).
- [13] R. Maier, Cooler synchrotron COSY - Performance and perspectives, *Nuclear Instruments and Methods in Physics Research, Section A: Accelerators, Spectrometers, Detectors and Associated Equipment* **390**, 1 (1997).
- [14] C. Weidemann, F. Rathmann, H. J. Stein, B. Lorentz, Z. Bagdasarian, L. Barion, S. Barsov, U. Bechstedt, S. Bertelli, D. Chiladze, G. Ciullo, M. Contalbrigo, S. Dymov, R. Engels, M. Gaisser, R. Gebel, P. Goslawski, K. Grigoriev, G. Guidoboni, A. Kacharava, V. Kamerdzhev, A. Khoukaz, A. Kulikov, A. Lehrach, P. Lenisa, N. Lomidze, G. Macharashvili, R. Maier, S. Martin, D. Mchedlishvili, H. O. Meyer, S. Merzliakov, M. Mielke, M. Mikirtychiants, S. Mikirtychiants, A. Nass, N. N. Nikolaev, D. Oellers, M. Papenbrock, A. Pesce, D. Prasuhn, M. Retzlaff, R. Schleichert, D. Schröer, H. Seyfarth, H. Soltner, M. Statera, E. Stefens, H. Stockhorst, H. Ströher, M. Tabidze, G. Tagliente, P. T. Engblom, S. Trusov, Yu. Valdau, A. Vasiliev, and P. Wüstner, Toward polarized antiprotons: Machine development for spin-filtering experiments, *Physical Review Special Topics - Accelerators and Beams* **18**, 020101 (2015).
- [15] G. Guidoboni, E. Stephenson, S. Andrianov, W. Augustyniak, Z. Bagdasarian, M. Bai, M. Baylac, W. Bernreuther, S. Bertelli, M. Berz, J. Böker, C. Böhme, J. Bsaisou, S. Chekmenev, D. Chiladze, G. Ciullo, M. Contalbrigo, J.-M. de Conto, S. Dymov, R. Engels, F. M. Esser, D. Eversmann, O. Felden, M. Gaisser, R. Gebel, H. Glückler, F. Goldenbaum, K. Grigoryev, D. Grzonka, T. Hahnrahts, D. Heberling, V. Hejny, N. Hempelmann, J. Hetzel, F. Hinder, R. Hipple, D. Hölscher, A. Ivanov, A. Kacharava, V. Kamerdzhev, B. Kamys, I. Keshelashvili, A. Khoukaz, I. Koop, H.-J. Krause, S. Krewald, A. Kulikov, A. Lehrach, P. Lenisa, N. Lomidze, B. Lorentz, P. Maanen, G. Macharashvili, A. Magiera, R. Maier, K. Makino, B. Mariański, D. Mchedlishvili, U.-G. Meißner, S. Mey, W. Morse, F. Müller, A. Nass, G. Natour, N. Nikolaev, M. Nioradze, K. Nowakowski, Y. Orlov, A. Pesce, D. Prasuhn, J. Pretz, F. Rathmann, J. Ritman, M. Rosenthal, Z. Rudy, A. Saleev, T. Sefzick, Y. Semertzidis, Y. Senichev, V. Shmakova, A. Silenko, M. Simon, J. Slim, H. Soltner, A. Stahl, R. Stassen, M. Statera, H. Stockhorst, H. Straatmann, H. Ströher, M. Tabidze, R. Talman, P. Thörngren Engblom, F. Trinkel, A. Trzciński, Yu. Uzikov, Yu. Valdau, E. Valetov, A. Vassiliev, C. Weidemann, C. Wilkin, A. Wrońska, P. Wüstner, M. Zakrzewska, P. Zuprański, and D. Zyuzin, How to Reach a Thousand-Second in-Plane Polarization Lifetime with 0.97-GeV/c Deuterons in a Storage Ring, *Physical Review Letters* **117**, 054801 (2016).
- [16] B. Hoistad, J. Ritman, *et al.*, Proposal for the Wide Angle Shower Apparatus (WASA) at COSY-Juelich - "WASA at COSY" (2004), arxiv:nucl-ex/0411038.
- [17] F. Müller, O. Javakhishvili, D. Shergelashvili, I. Keshelashvili, D. Mchedlishvili, F. Abusaif, A. Aggarwal, L. Barion, S. Basile, J. Böker, N. Canale, G. Ciullo, S. Dymov, O. Felden, M. Gagoshidze, R. Gebel, N. Demary, K. Grigoryev, D. Grzonka, T. Hahnrahts, V. Hejny, A. Kacharava, V. Kamerdzhev, S. Karanth, A. Kulikov, A. Lehrach, P. Lenisa, N. Lomidze, B. Lorentz, G. Macharashvili, A. Magiera, Z. Metreveli, A. Nass, N. N. Nikolaev, M. Nioradze, A. Pesce, V. Poncza, D. Prasuhn, J. Pretz, F. Rathmann, A. Saleev, T. Sefzick, Y. Senichev, V. Shmakova, J. Slim, H. Soltner, E. Stephenson, H. Ströher, M. Tabidze, G. Tagliente, Y. Uzikov, Y. Valdau, T. Wagner, A. Wrońska, P. Wüstner, and M. Żurek, A new beam polarimeter at COSY to search for electric dipole moments of charged particles, *Journal of Instrumentation* **15** (12), P12005.
- [18] H. Kleines, K. Zwill, P. Wüstner, W. Erven, P. Kammerling, G. Kemmerling, H.-W. Loevenich, A. Ackens, M. Wolke, V. Hejny, H. Ohm, T. Sefzick, R. Nellen, P. Marciniowski, K. Fransson, L. Gustafsson, A. Kupsc, and H. Calen, The new DAQ system for WASA at COSY, *IEEE Transactions on Nuclear Science* **53**, 893 (2006).
- [19] R. A. Light, Mosquitto: Server and client implementation of the MQTT protocol, *Journal of Open Source Software* **2**, 265 (2017).
- [20] L. Dalesio, A. Kozubal, and M. Kraimer, EPICS Architecture, in *3rd International Conference on Accelerator and Large Experimental Physics Control Systems (ICALPCS'91)*, Tsukuba, Japan, 11-15 November 1991 (JACOW Publishing, Geneva, Switzerland, 1992) pp. 278-282.
- [21] N. N. Nikolaev, F. Rathmann, J. Slim, A. Andres, V. Hejny, A. Nass, A. Kacharava, P. Lenisa, J. Pretz, A. Saleev, V. Shmakova, H. Soltner, F. Abusaif, A. Aggarwal, A. Aksentev, B. Alberdi, L. Barion, I. Bekman, M. Beyß, C. Böhme, B. Breitkreutz, N. Canale, G. Ciullo, S. Dymov, N.-O. Fröhlich, R. Gebel, M. Gaisser, K. Grigoryev, D. Grzonka, J. Hetzel, O. Javakhishvili, V. Kamerdzhev, S. Karanth, I. Keshelashvili, A. Kononov, K. Laihem, A. Lehrach, N. Lomidze, B. Lorentz, G. Macharashvili, A. Magiera, D. Mchedlishvili, A. Melnikov, F. Müller, A. Pesce, V. Poncza, D. Prasuhn, D. Shergelashvili, N. Shurkhno, S. Siddique, A. Silenko, S. Stassen, E. J. Stephenson, H. Ströher, M. Tabidze, G. Tagliente, Y. Valdau, M. Vitz, T. Wagner, A. Wirzba, A. Wrońska, P. Wüstner, and M. Żurek, Spin decoherence and off-resonance behavior of radio-frequency-driven spin rotations in storage rings, *Physical Review Accelerators and Beams* **27**, 111002 (2024).